International Journal of Mechanical and Production Engineering Research and Development (IJMPERD)
ISSN (P): 2249-6890; ISSN (E): 2249-8001
Vol. 8, Issue 5, Oct 2018, 271-280

NONLINEAR FINITE ELEMENT SIMULATION OF FRICTION STIR WELDING OF AA7075 T651 ALUMINIUM ALLOY

MD. PARWEZ ALAM[1] & AMAR NATH SINHA[2]

[1]*Research Scholar, Department of Mechanical Engineering, National Institute of Technology, Patna, India*

[2]*Professor, Department of Mechanical Engineering, National Institute of Technology, Patna, India*

ABSTRACT

Friction Stir Welding (FSW) is a solid state joining process. Heat generation and heat distribution of friction stir welding is a fundamental phenomenon and Sound welding is dependent on the adequate heat generation. Due to stirring of materials it is difficult to measure temperature in stir zone. Numerical simulation helps in finding the temperature in stir zone. Numerical simulation of the temperature distribution of friction stir welding of aluminium alloy has been investigated in the present research. A finite element code using ANSYS APDL software package has been developed for modelling of friction stir welding. Thermal physical properties of the material aluminium alloy are considered as temperature dependent in the present work. The cooling effect caused by the free convection in ambient air, backing plate and clamped bar is taken into account. It was observed that the peak temperature is not uniform along weld line, inhomogeneous temperature distribution along thickness.

KEYWORDS: Friction Stir Welding, ANSYS, Friction Coefficient, Heat Generation & Temperature Distribution

Received: Jun 27, 2018; **Accepted**: Aug 17, 2018; **Published**: Sep 06, 2018; **Paper Id.**: IJMPERDOCT201830

Original Article

1. INTRODUCTION

Welding is an essential phenomenon in the manufacturing sector because it is impossible to produce all complex components. There are various welding processes are applied in different application. Friction stir welding is a widely growing technology due its smooth, precise and effective operation. It was invented in the 1991 by Wayne Thomas and his colleagues of The Welding Institute (TWI) at Cambridge, U. K. [1]. The FSW process performs below the melting point of the material so it is kept in the solid state welding process. In this welding, there is no requirement of filler material. It is also free from fumes, arc flash, spatter and pollution are associated with most of the conventional welding. It is also known as green welding. Some welding defects such as shrinkage, cracking and porosity are generally associated with conventional welding process, but FSW is free from aforementioned defects and characteristics of welded plate remain almost same as that of the base metal [2].

Many researchers have been working in the area of numerical simulation of friction stir welding for determining temperature distribution by using different heat source. Based on literature survey, FSW modelling may be divided into three main categories; (a) finite element based models, (b) pure analytical thermal models, and (c) computational fluid dynamics models [3].

Frictional heat, which is generated due to tool sliding over the workpiece, was considered as a major heat source during FSW [4]. A 3-D thermal and thermo mechanical FEM model for FSW was developed by Chao et al. [5] with considering only frictional heat as the heat source. But, H. B. Schmidt et al., [6] introduced contact

condition between tool and workpiece by a parameter called slip rate (δ). It is varies from 0 to 1. The value 0 indicates for sliding and only friction is responsible for heat, whereas the value 1 indicates the contact condition is sticking and only shear deformation generates heat. Heat generation in FSW is directly proportional to plastic deformation and frictional heat created during the welding process [7].

Frictional contact heat and the plastic deformational heat were considered as a heat source in modelling of friction stir welding [8]. Li & Liu, [9] applied external heat source for the heat generation from tool movement instead of heat generation by friction or plastic deformation. They reported that the temperature dependent heat transfer coefficient and contact pressure significantly affect the thermal analysis.

Quality of weld depends on adequate heat. Determination of heat generation and distribution are very important, but temperature measurement is difficult in stir zone. Numerical modelling is a good alternative to measure temperature in this zone. Numerical modelling saves time and money. Since several phenomena occur simultaneously during friction stir welding. All these make synergetic effect during the welding. So, better understanding of physics is required. Concept of physics play important role in problem solving. This also makes interesting for researchers to achieve proper results as experimental value. Figure 1 shows a schematic diagram of friction stir welding.

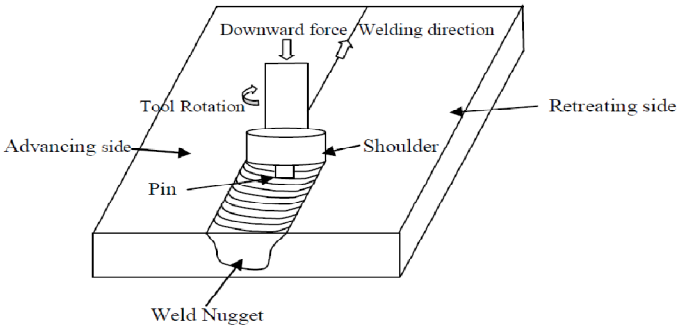

Figure 1: Schematic Diagram of Friction Stir Welding

There are several process parameters responsible for heat generation during FSW. Rotational speed, Welding speed, force, plunge depth and speed, shoulder profile and size, tool pin diameter and length, tilt angle and material properties are some of them.

2 COMPUTATIONAL PROCEDURE

2.1 Problem Definition

As mentioned above, the present investigation aims to develop a model in finite element software ANSYS APDL to estimate heat generation due to friction during friction stir welding and study the temperature distribution along the thickness of the plate, along the welding line, and along the perpendicular to weld direction.

2.2 Material Model

Friction stir welding tool is considered as rigid body while the workpiece is considered as ductile body. Aluminium alloy 7075 T651 is considered for experimental work so; similar thermo mechanical properties are specified. Thermal conductivity, specific heat, and density are considered as temperature dependent and Poisson's ratio, coefficient of thermal expansion is considered as temperature independent properties in this model. It is also assumed that the workpiece behave as the rate-independent plastic material. Material properties are given in the figure 2.

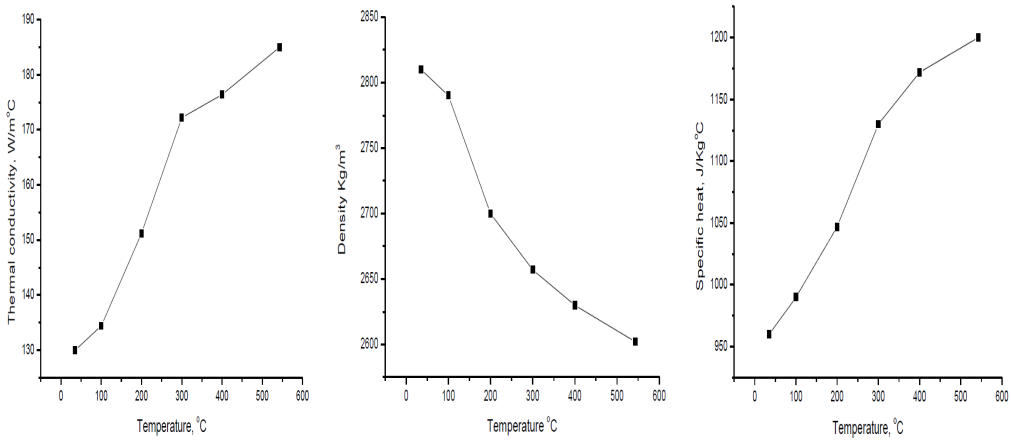

Figure 2: Temperature Dependent Physical Properties of AA7075T651

2.3 Frictional Contact Behaviour

According to coulomb's law, two contacting bodies remain at rest up to a certain value of shear stress. This condition is known as sticking condition. When the value of shear stress exceeds then the body will slide. In sliding condition, the tool surface and the workpiece surface slides on each other. Mathematically it is expressed as equation (1)

$$\tau = \mu p = \mu\sigma \tag{1}$$

Where, p, μ, and σ is contact normal pressure, friction coefficient and contact stress respectively.

In sticking condition, matrix segment of workpiece sticks with the rotating tool and rotated with tool. The velocity difference between stationary of material and material moving with tool is considered as shear stress. The maximum shear stress for yielding was assumed as

$$\tau = \frac{\sigma y}{\sqrt{3}} = 0.577\sigma_y \tag{2}$$

Where, yield strength of material. If contact shear stress is less than the value of 0.577 σ_y behaves as sticking condition. In this model temperature dependent friction coefficient is used which vary 0.3 to 0.01 [10]. Figure 3 shows the modified coulomb's law.

2.4 Thermal and Mechanical Boundary Condition

In thermal boundary condition Fourier's law is applied to heat conduction in plate and heat convection is applied for heat loss to ambient and contacting surface.

The initial boundary condition for this model is used as

$$T(x, y, z, t) = T_o \tag{3}$$

Where T_o is the ambient temperature at time t=0 and T (x, y, z, t) represents the transient temperature field T, which is a function of time t and spatial coordinate (x, y, z).

In friction stir welding heat is generated by friction plastic deformation, whereas heat transfer during friction stir welding is a typical nonlinear instant heat conduction process which is governed by the Fourier law of heat conduction. It is expressed as equation (4)

$$\frac{\partial}{\partial x}\left(Kx\frac{\partial T}{\partial x}\right)+\frac{\partial}{\partial y}\left(Ky\frac{\partial T}{\partial y}\right)+\left(Kz\frac{\partial T}{\partial z}\right)+\dot{Q}=\rho Cp(\frac{\partial T}{\partial t}) \quad (4)$$

Where, ρ, Cp, K and $\dot{Q}$represents density, Specific heat, directional thermal conductivity and rate of heat generation respectively.

In the present simulation only convective heat transfer is considered. The heat loss from free surfaces of the workpiece and the tool are calculated as equation (5)

$$q_1= h_f (T-T_o) \quad (5)$$

where, T, T_o and h_f refers absolute temperature of the workpiece, ambient temperature and convection coefficient of free surfaces of the workpiece and the tool. Value of heat transfer coefficient for aluminium alloy to air is taken 30 W/m^2.

The backing plate is always contact with the lower surface of the workpiece and act as a heat sink. It is found that most of heat is lost through the backing plate. For simplicity, it is modelled as a convection condition and considered a higher convection coefficient. The value of heat transfer coefficient is taken as 100 W/m^2 and expressed as equation (6)

$$q_2= h_b (T-T_o) \quad (6)$$

where, h_b refers convection coefficient of the lower surface of the workpiece and backing plate. In addition, Workpiece is clamped as similar as experimental setup(see figure 8) and during the welding, the workpiece is intimate contact of with the clamping bar. It is also modelled as a convection condition and the heat transfer coefficient is taken 50 W/m^2

$$q_3= h_c (T-T_o) \quad (7)$$

Where, h_c refers convection coefficient of the workpiece surface and clamping bar. In this modelling radiation loss are not considered.

The mechanical boundary condition applied as a clamping bar on plate and bottom support. The bottom portion of the workpiece is a constraint in normal direction and taken us = 0. Whereas clamped portion is taken as complete restraint as real i. e. there is no movement in any direction. $U_x = U_y = U_z = 0$ is applied. Thermal and mechanical boundary condition is shown in Figure 4.

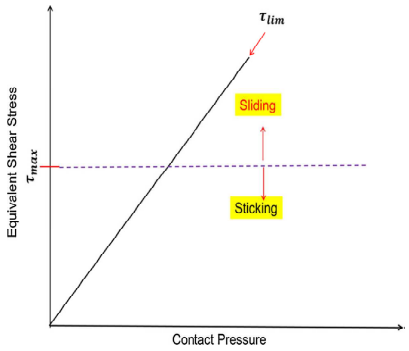

Figure 3:Modified Coulomb's Law for Sliding and Sticking Condition [10]

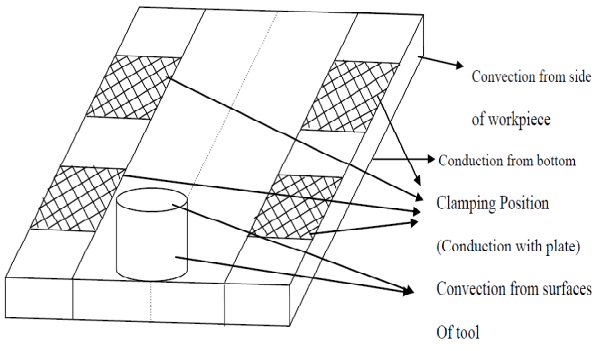

Figure 4: Boundary Condition of Plates and Tool

3. MODEL DESCRIPTION

Two rectangular plates with dimension 60 mm × 50mm × 3.18 mm were created and meshed. For accurate results, finer mesh is created along the weld line. Total number of nodes and elements are 7759 and 7755 respectively. A rigid tool, without pin is created on the weld joint. Selection of the element in ANSYS APDL is an important parameter. In this analysis, 3D 20 node couple field element SOLID226 was selected because it is capable to large strain capabilities, large deflection, stress stiffness and plasticity. It is shown in figure 5. Since SOLID226 consists midside node which can lead (a) oscillation in the thermal solution & (b) non physical temperature distribution. Therefore, in this analysis midside node is deleted to avoid these phenomena.

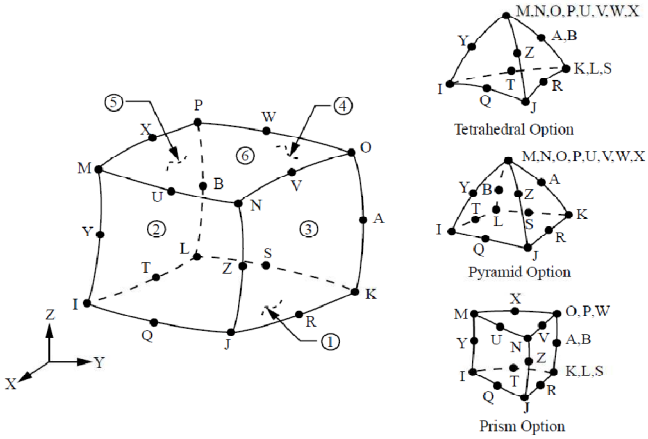

Figure 5: SOLID226 [12]

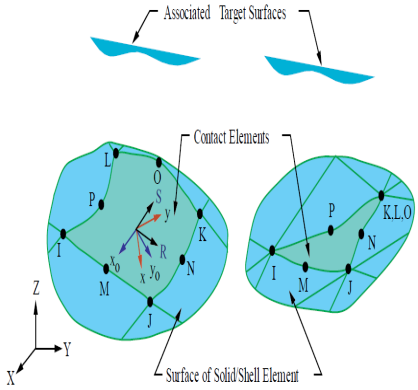

Figure 6: CONTA174 and TARGE170 [12]

For analysing transient effect of friction stir welding Lagrangian model is applied. In this model tool is moved from one end of the workpiece and reached at the other end. Each location experienced individual thermal history during this movement.

Contact behaviour is properly defined between various parts. In this model it is defined between (a) The plates (b) the pilot node and tool (c) The tool and work plate. Contact pair between the plates is defined by using 3D 8 node surface to surface contact element CONTA174. Hence it is applicable to 3D structural & couple field contact analysis. It is also noted that 3D target element TARGE170 is used for pair based contact. Figure 5 shows CONTA174 and TARGE170 element.

Since the FSW process is a highly nonlinear so, surface projection based contact method is defined at the contact interface. The bonding temperature between plates is taken 400℃. It was applied as a real constant TBND for CONTA174. This value shows that when temperature reaches or exceeds 400℃ then the contact type of behaviour changed into bonded type and remains in bonded even thoughthe temperature decreases to below the bonding value. Another important real constant thermal contact conductance (TCC) is used between contact interfaces of plates. A high value 2×10^6 is taken for perfect conduction of temperature between the plates. Mathematics TCC is expressed as equation (8)

$$q = T_{cc} (q_t - q_c) \quad (8)$$

Where q is heat flux per unit area, T_{cc} thermal contact conductance, q_c& q_t is contact parts on target and contact surfaces.

As previously discussed, the tool is rotated and moves along the weld line from one end to another. This rotational and translation movement of the tool is controlled by a pilot node which is created on the top surface of the tool. A multipoint constraint (MPC) algorithm with contact surface behaviour defined as bonded always is used to constrain the contact nodes to the rigid body motion defined by the pilot node.

Again, CONTA174 & TARGE170 is used for defining contact pair between the workpiece and the tool respectively. Here the workpiece is considered as deformable bodies, whereas tool is rigid. Coupled transient thermal-structural analysis is performed because heat is generated due to frictional dissipated energy. Two real constant FHTG and FWGT required for this analysis.

The rate of frictional dissipated energy is mathematically expressed as;

$$q = FHTG \times \tau XV \quad (9)$$

Where, FHTG is the fraction of friction energy converted into heat. In this analysis FHTG is taken 1 for 100% frictional energy converted into heat. T IS equivalent frictional stress and V is sliding rate.

Heat generated during frictional contact is distributed in the tool (Target side, q_t) and the workpiece (Contact side, q_c). It is defined by real constant FWGT (Heat distribution weighing factor). This is expressed as

$$qc = FWGT \times FHTG\ \tau \times V \quad (10)$$

$$qt = (1 - FWGT) \times FHTG\ \tau \times V \quad (11)$$

In this analysis 5 % of generated heat was distributed in tool and remaining in workpiece.

It is considered that only 80% of plastic heat deformation converts into heat. Mathematically it is expressed as,

$$q_p = 0.8\ X\ \text{plastic work} = 0.8 \int_0^t \{\sigma\}^T [M]\{d\varepsilon^{pl}\} \quad (12)$$

This simulation contains four load steps as plunge, dwell, traverse and pull out of the tool. Automatic time step is activated for faster solution. Newton Raphson technique was utilized to solve the governing non-linear equation.

4. EXPERIMENTAL PROCEDURE

AA7075 T651 plates with dimension with 120mm length and 100 mm width and 3 mm thick were used in this study. The workpieces were polished with acetone and kept on backing plate which is made up of mild steel with 25 mm thickness, and clamped rigidly by clamping bar to prevent movement in any direction. Heat treated cylindrical tool of 2.7 mm height with 0°tilt angle is employed for this analysis.

Figure 7: Experimental setup of FSW [Courtesy by TRTC, Patna]

Figure 8: FSW Tool

Table 1 Tool Details and Material Properties

Pin Diameter (mm)	Shoulder Diameter (mm)	Youngs Modulus (GPa)	Poisson's Ratio	Thermal Conductivity (W/m°C)	Specific Heat (J/kg°C)	Density (kg/m^3)
4 mm	15	210	0.3	24.4	460	7750

The temperature were measured with 16 K- type thermocouples with a sheath diameter of 1.5 mm. Small holes with diameter of 1.5 mm were drilled into plates at 1.8 mm at a different distance from the weld line. Experimental setup and FSW tool are shown in figure 6 and figure 7 respectively. Details of tool are given in table 1.

5. RESULTS AND DISCUSSIONS

A 3 D modelling is developed for analyzing thermal history during friction stir welding by the help of ANSYS APDL and similar results were found as previous [10]. Figure 6 shows temperature distribution during welding.

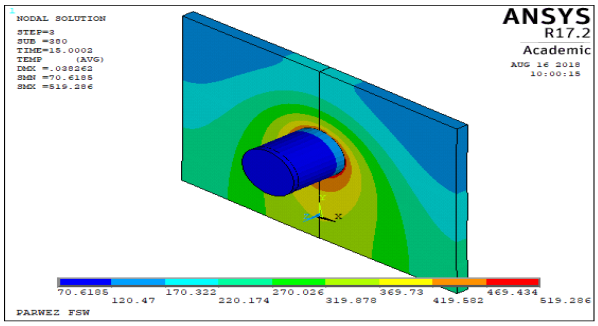

Figure 9: Temperature Distribution in ANSYS

In this modelling tool is penetrated without rotating hence there is no heat generated during plunging stage but in the dwell or preheat periods tool rotates with 300 rpm. In this analysis 5 second is taken for dwell period. After dwell period tool moves along weld line. Three points (X, Y) = (0, 0) mm, X, Y= (0, 30)mm and X, Y=(0,60) mm on weld line is taken for analyzing temperature distribution. It was observed that the all three points experienced different peak temperature. It is due to friction coefficient between the tool and the workpiece. As temperature increases the value of friction coefficient decreased and vice versa. It is also observed that peak temperature remains for some time because of tool shoulder takes some time to leave that specified nodes

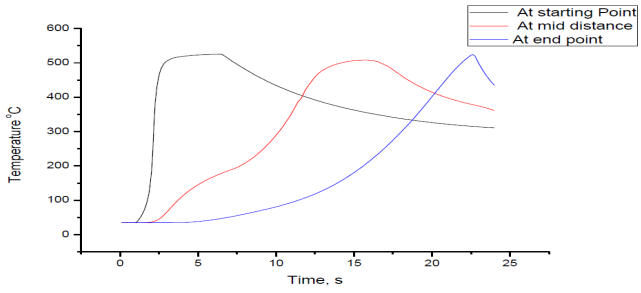

Figure 10: Temperature Distribution along Weld Line of Friction Stir Welding

Similarly, six points are chosen for analyzing temperature distribution along the perpendicular to the weld direction. These points are shown in table 2. It is observed that the temperature difference between X_1, X_2 and X_3 at Y=0 mm is more than Y=60 mm. figure 10 and 11 is show the temperature distribution of X_1, X_2, X_3 point at Y=0 mm and Y=60 mm.

Table 2: Temperature Analyzing Position

	X_1 (Weld Centre)	X_2 (Just beyond shoulder)	X_3(Far from welding)
At Y=0 mm	0 mm	7.6 mm	14 mm
At Y=60 mm	0 mm	7.6 mm	14 mm

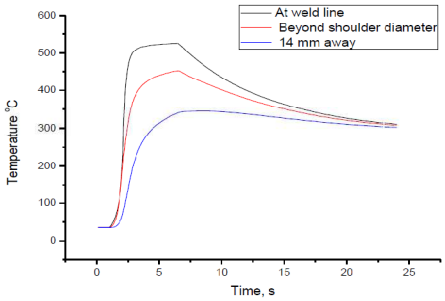

Figure 11: Temperature Distribution away from Weld Line at Y=0

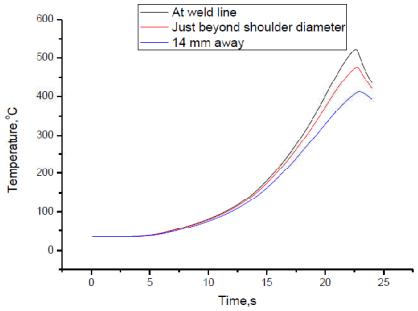

Figure 12: Temperature Distribution away from Weld Line at Y=60 mm

In homogeneous heat distribution was found along the thickness of weld plate. Top surface of the workpiece experiences more heat due frictional contact of the tool whereas, bottom surface loss more heat because of backing plate act as a heat sink. It is also observed that the bottom surface of weld joint becomes weaker than the top surface. In addition, it is also observed that the temperature sharply increased to peak point and remains for some instant and gradually decreases.

6. CONCLUSIONS

A three-dimensional finite element model using ANSYS APDL software has been developed to study the temperature distribution in AA7075T651. From this model following conclusion can be made:

- Temperature is not uniform throughout the welding line. It is fluctuated due to friction coefficient.
- Temperature is measured three point points as x=0 mm, x= 7.6 mm and x= 14 mm and compare the temperature difference at beginning point and end point and it is found that the beginning point experiences more temperature differences.
- Inhomogeneous temperature is found along the weld thickness. Faying surface experienced more temperature than bottom surface.
- It is also observed that during the welding temperature sharply increased and remains for some instant and gradually decreases.

7. ACKNOWLEDGMENTS

This work was supported by NIT Patna. I thank for its support in providing facility for accessing different Journals of friction stir welding and ANSYS software package.

REFERENCES

1. *Thomas, W. M., Nicholas, E. D., Needam, J. C., Murch, M. G., Templesmith, P., & Dawes, C. J. (1995). GB Patent Application No. 9125978.8, December 1991 and US Patent No. 5460317. October.*
2. *Gibson, B. T., Lammlein, D. H., Prater, T. J., Longhurst, W. R., Cox, C. D., Ballun, M. C.,... & Strauss, A. M. (2014). Friction stir welding: process, automation, and control. Journal of Manufacturing Processes, 16(1), 56-73.*
3. *Aziz, S. B., Dewan, M. W., Huggett, D. J., Wahab, M. A., Okeil, A. M., & Liao, T. W. (2016). Impact of Friction Stir Welding (FSW) process parameters on thermal modeling and heat generation of aluminum alloy joints. Acta Metallurgica Sinica (English Letters), 29(9), 869-883.*
4. *Noble Chen, C., & Kovacevic, R. (2004). Thermomechanical modelling and force analysis of friction stir welding by the finite element method. Proceedings of the Institution of Mechanical Engineers, Part C: Journal of Mechanical Engineering Science, 218(5), 509-519.*
5. *Chao, Y. J., & Qi, X. (1998). Thermal and thermo-mechanical modeling of friction stir welding of aluminum alloy 6061-T6. Journal of materials processing and manufacturing science, 7, 215-233.*
6. *Schmidt, H., Hattel, J., & Wert, J. (2003). An analytical model for the heat generation in friction stir welding. Modelling and Simulation in Materials Science and Engineering, 12(1), 143.*
7. *Buffa, G., Hua, J., Shivpuri, R., & Fratini, L. (2006). A continuum based fem model for friction stir welding—model development. Materials Science and Engineering: A, 419(1-2), 389-396.*
8. *Dong, P., Lu, F., Hong, J. K., & Cao, Z. (2001). Coupled thermomechanical analysis of friction stir welding process using simplified models. Science and Technology of Welding and Joining, 6(5), 281-287..*
9. *Rao, G. A., Reddy, G. C. M., & Kumar, G. S. R. Multi Response Objective Optimization Of Friction Stir Welding Parameters Of Dissimilar Metals Of Aa 6061 Aluminumand Is319 Brass Joining Through Taguchi's Method.*
10. *Li, H., & Liu, D. (2014). Simplified Thermo-Mechanical Modeling of Friction Stir Welding with a Sequential FE Method. International Journal of Modeling and Optimization, 4(5), 410.*
11. *Aziz, S. B., Dewan, M. W., Huggett, D. J., Wahab, M. A., Okeil, A. M., & Liao, T. W. (2018). A Fully Coupled Thermomechanical Model of Friction Stir Welding (FSW) and Numerical Studies on Process Parameters of Lightweight Aluminum Alloy Joints. Acta Metallurgica Sinica (English letters), 31(1), 1-18.*
12. *Fratini, L., Buffa, G., & Shivpuri, R. (2010). Mechanical and metallurgical effects of in process cooling during friction stir welding of AA7075-T6 butt joints. Acta Materialia, 58(6), 2056-2067.*
13. *Ansys Inc., ANSYS Mechanical APDL Theory Reference.*